Atmos. Chem. Phys., 8, 6565–6576, 2008
www.atmos-chem-phys.net/8/6565/2008/
© Author(s) 2008. This work is distributed under
the Creative Commons Attribution 3.0 License.

Atmospheric Chemistry and Physics

FRESCO+: an improved O_2 A-band cloud retrieval algorithm for tropospheric trace gas retrievals

P. Wang[1], **P. Stammes**[1], **R. van der A**[1], **G. Pinardi**[2], **and M. van Roozendael**[2]

[1]Royal Netherlands Meteorological Institute (KNMI), De Bilt, The Netherlands
[2]BIRA-IASB, Belgian Institute for Space Aeronomy, Brussels, Belgium

Received: 21 February 2008 – Published in Atmos. Chem. Phys. Discuss.: 27 May 2008
Revised: 20 August 2008 – Accepted: 22 September 2008 – Published: 14 November 2008

Abstract. The FRESCO (Fast Retrieval Scheme for Clouds from the Oxygen A-band) algorithm has been used to retrieve cloud information from measurements of the O_2 A-band around 760 nm by GOME, SCIAMACHY and GOME-2. The cloud parameters retrieved by FRESCO are the effective cloud fraction and cloud pressure, which are used for cloud correction in the retrieval of trace gases like O_3 and NO_2. To improve the cloud pressure retrieval for partly cloudy scenes, single Rayleigh scattering has been included in an improved version of the algorithm, called FRESCO+. We compared FRESCO+ and FRESCO effective cloud fractions and cloud pressures using simulated spectra and one month of GOME measured spectra. As expected, FRESCO+ gives more reliable cloud pressures over partly cloudy pixels. Simulations and comparisons with ground-based radar/lidar measurements of clouds show that the FRESCO+ cloud pressure is about the optical midlevel of the cloud. Globally averaged, the FRESCO+ cloud pressure is about 50 hPa higher than the FRESCO cloud pressure, while the FRESCO+ effective cloud fraction is about 0.01 larger.

The effect of FRESCO+ cloud parameters on O_3 and NO_2 vertical column density (VCD) retrievals is studied using SCIAMACHY data and ground-based DOAS measurements. We find that the FRESCO+ algorithm has a significant effect on tropospheric NO_2 retrievals but a minor effect on total O_3 retrievals. The retrieved SCIAMACHY tropospheric NO_2 VCDs using FRESCO+ cloud parameters (v1.1) are lower than the tropospheric NO_2 VCDs which used FRESCO cloud parameters (v1.04), in particular over heavily polluted areas with low clouds. The difference between SCIAMACHY tropospheric NO_2 VCDs v1.1 and ground-based MAXDOAS measurements performed in Cabauw, The Netherlands, during the DANDELIONS campaign is about -2.12×10^{14} molec cm^{-2}.

Correspondence to: P. Wang
(wangp@knmi.nl)

1 Introduction

Clouds have significant effects on trace gas retrievals from satellite spectrometers operating in the UV/visible, such as GOME, SCIAMACHY, OMI and GOME-2. Clouds can shield trace gases from observation, but they can also enhance the sensitivity to trace gases above the clouds. Because of the relatively coarse spatial resolution of the above satellite instruments, only 5–15% of the pixels are cloud-free (Krijger et al., 2007). To correct for cloud effects on trace gas retrievals, the most relevant cloud parameters are the cloud fraction and height (Stammes et al., 2008). There are several cloud retrieval algorithms that have been developed for GOME and SCIAMACHY using the O_2 A-band (Koelemeijer et al., 2001; Kokhanovsky et al., 2006; van Diedenhoven et al., 2007) or using Polarisation Monitoring Devices (PMDs) (Grzegorski et al., 2006; Loyola, 2004). FRESCO (Koelemeijer et al., 2001) is a simple, fast and robust algorithm, which is also implemented in GOME-2 level 1 data processor (Munro and Eisinger, 2004).

In the FRESCO algorithm, the cloud pressure and the effective cloud fraction are retrieved from top-of-atmosphere (TOA) reflectances in three 1-nm wide wavelength windows at 758–759, 760–761, and 765–766 nm. The cloud is assumed to be a Lambertian surface with albedo 0.8, and only absorption due to O_2 above the cloud and the ground surface and reflections from the surface and cloud are taken into

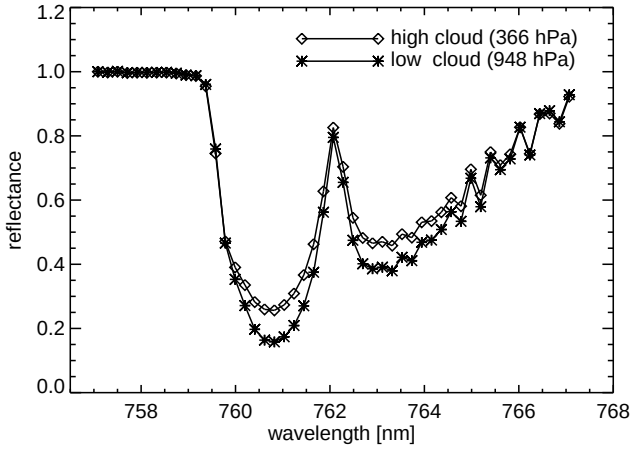

Fig. 1. Typical O_2 A-band spectra measured by GOME. The spectra are normalized at 758 nm to show the relative depth of the band for clouds at different heights.

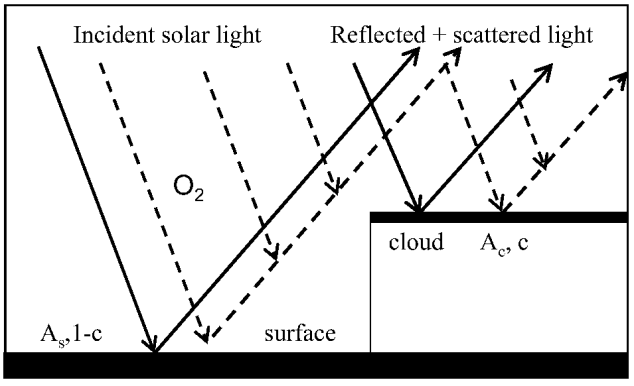

Fig. 2. Atmospheric radiation model used in FRESCO+. The cloud and surface are both assumed to be Lambertian reflectors. Three light paths are considered: (1) from sun to surface to satellite, (2) from sun to cloud to satellite, (3) from sun to atmosphere to satellite according to single Rayleigh scattering. (1)+(2): solid lines, (3): dashed lines. Along all three paths O_2 absorption and Rayleigh scattering extinction are included in the forward model simulation.

account. The FRESCO effective cloud fractions and cloud pressures have been validated globally and regionally, and the products have been used in trace gas retrievals (Koelemeijer et al., 2003; Tuinder et al., 2004; Grzegorski et al., 2006; Fournier et al., 2006).

The effective cloud fraction retrieved by FRESCO is the cloud fraction of a Lambertian cloud with albedo 0.8 yielding the same TOA radiance as the real cloud in the scene. Generally the effective cloud fraction is smaller than the geometric cloud fraction. The choice of Lambertian cloud albedo 0.8 and effective cloud fraction concept have recently been discussed by Stammes et al. (2008). The use of effective cloud fractions for the cloud correction in the O_3 and NO_2 retrievals has been investigated in several papers (Koelemeijer and Stammes, 1999; Wang et al., 2006; Stammes et al., 2008). The Lambertian cloud is a good approximation for cloud correction of total O_3 column retrievals. For scenes with 50% cloud coverage the error in the total O_3 column due to the Lambertian cloud assumption instead of a scattering cloud model is about 0.5% (Stammes et al., 2008). For tropospheric NO_2 retrievals, the effective cloud fraction assumption leads to errors of about 10% (Wang et al., 2006). Here the cloud height is also important, because the large amount of tropospheric NO_2 can be inside the clouds or below the clouds.

Recently, we have found that the FRESCO cloud pressures are often too low (cloud heights are too high) when the effective cloud fractions are less than 0.1. These are cases with a relatively large contribution from Rayleigh scattering, which is missing in the FRESCO algorithm. Apparently, the missing Rayleigh scattering is compensated by fitting a high cloud. Pixels with small cloud fractions are important for tropospheric trace gas retrievals. For example, in the operational tropospheric NO_2 retrievals from the TEMIS project the effective cloud fractions are allowed to be less than 0.3 (Eskes and Boersma, 2003). Therefore, we improved the FRESCO algorithm by the addition of single Rayleigh scattering in the transmission and reflectance databases (forward calculations) and in the retrieval. This improved version is called FRESCO+.

The structure of the paper is as follows. In Sect. 2 we explain the principle of FRESCO+. The formulas of FRESCO+ are given in the Appendix. The FRESCO+ results and the comparisons with FRESCO are shown in Sect. 3 for simulations and real data. In Sect. 4 the effects of FRESCO+ cloud parameters on O_3 and NO_2 vertical column density (VCD) retrievals are discussed. The SCIAMACHY NO_2 VCDs using FRESCO+ and FRESCO cloud corrections are compared with NO_2 VCD from ground-based MAXDOAS measurements. Sect. 5 contains the conclusions.

2 Principle of FRESCO+

The FRESCO+ algorithm retrieves the effective cloud fraction (c_{eff}) and cloud pressure (P_c) from the TOA reflectance at three 1-nm wide windows, namely 758–759, 760–761 and 765–766 nm. Each of the three windows contains 5 reflectance measurements (spectral data points). Due to the presence of clouds, the reflectance in the continuum window (758 nm) is larger than for a clear sky scene, whereas the depth of the strongest O_2 absorption band at 760 nm and of the weaker O_2 absorption band at 765 nm varies according to the height and the optical thickness of the cloud. Typical O_2 A-band spectra of scenes with high and low clouds measured by GOME are shown in Fig. 1.

The atmospheric radiation model assumed in the FRESCO+ algorithm is shown in Fig. 2. The FRESCO+ algorithm fits a simulated reflectance spectrum to the measured reflectance spectrum in the three windows, to retrieve the effective cloud fraction and cloud pressure. The simulated reflectance ($R_{\rm sim}$) at TOA is written as the sum of the reflectances of the cloud-free and cloudy parts of the pixel:

$$R_{\rm sim} = (1-c)T_s A_s + (1-c)R_s + cT_c A_c + cR_c. \qquad (1)$$

Here R_c, T_c and R_s, T_s are the single Rayleigh scattering reflectance and transmittance of the cloudy and cloud-free part of the pixel, respectively. T_c and T_s contain O_2 absorption and Rayleigh scattering extinction, and are pre-calculated as a function of the solar zenith angle (SZA), viewing zenith angle (VZA), wavelength, and altitude. A_c is the cloud albedo, which is assumed to be 0.8, and A_s is the surface albedo taken from a climatology (Koelemeijer et al., 2003; Fournier et al., 2006). The surface pressure is calculated from surface elevation. The O_2 transmission is calculated using a line-by-line method for a 1-pm wavelength grid using the line parameters from HITRAN 2004 (Rothman et al., 2005) and then convolved using the instrument response function at the measurement wavelength grid. Rayleigh scattering is a small but significant contribution to $R_{\rm sim}$ in the case of an almost cloud-free pixel. Due to single Rayleigh scattering the reflectance at 760 nm is larger than if only surface or cloud reflection would take place, while at 758 nm the reflectance is a bit smaller than without single Rayleigh scattering. The single Rayleigh scattering reflectances are pre-calculated and stored as a look-up-table (LUT) which has the same format as the transmission database. The Rayleigh scattering formulae used in FRESCO+ are given in the Appendix, whereas the O_2 transmission formulae are given in detail by Wang and Stammes (2007).

3 Simulation, application and validation of FRESCO+

3.1 FRESCO+ and FRESCO cloud retrievals from simulated spectra

To test the FRESCO+ algorithm on simulated spectra of cloudy scenes, O_2 A-band reflectance spectra were simulated with the DAK (Doubling-Adding KNMI) model (De Haan et al., 1987; Stammes et al., 1989; Stammes, 2001). DAK is a line-by-line radiative transfer model in which multiple scattering is fully taken into account. The simulations are performed for a mid-latitude-summer atmosphere consisting of 32 plane-parallel homogeneous layers with Rayleigh scattering and oxygen absorption. In this atmosphere homogeneous scattering cloud layers are inserted, with varying optical thickness and height. The cloud particle scattering phase function is a Henyey-Greenstein function with asymmetry parameter 0.85. The cloud scenes are simulated for single-layer clouds and two-layer clouds. For the single-layer cloud case, the cloud is at 7–8 km, the cloud optical thickness is 7 and the geometric cloud fraction is 0.5 and 1. The two-layer cloud case includes two cloud scenes, namely optically thin and optically thick clouds. For the optically thin clouds, the first cloud layer is at 9–10 km with optical thickness 7, and the second cloud layer is at 1–2 km, with optical thickness 14. For the optically thick clouds, the cloud layers are at the same altitude as the optically thin cloud, but the cloud optical thickness is 14 for the first layer and 21 for the second layer. In all the simulations the surface albedo (A_s) is 0.1, the surface height is 0 km and no aerosol is included. We also simulated O_2 A-band reflectance spectra for a cloud-free scene to obtain reflectance spectra for partly cloudy scenes, by using the independent-pixel-approximation. The O_2 absorption cross-sections were calculated line-by-line using HITRAN 2004 line parameters, which is the same in FRESCO+ and FRESCO. For reason of comparison, the FRESCO algorithm (without Rayleigh scattering) was included in the tests. The spectra were calculated from 755 to 772 nm at 0.01 nm wavelength grid, and then convoluted with the SCIAMACHY slit function. The geometries used in the retrievals are: nadir view, and solar zenith angles (SZA) 0, 30, 45, 60, 70, and 75 degrees.

First we consider cloud-free scenes. The effective cloud fractions retrieved by FRESCO and FRESCO+ from the simulated clear sky spectra were almost 0 (less than 0.01). However, the cloud height retrieved by FRESCO was close to 8 km. The reason for this large cloud height is that Rayleigh scattering by air molecules is included in the DAK model, but not in FRESCO. So the reflectances inside the O_2 A-band (at 760 and 765 nm) are larger than that of a purely absorbing O_2 atmosphere. Using the same clear sky DAK spectra as input, the cloud heights retrieved by FRESCO+ are about 0.5 km, which is much more reasonable than the FRESCO cloud height. So we may expect that FRESCO+ will give better cloud height results for partly cloudy scenes than FRESCO. The remaining 0.5 km error in cloud height for the cloud free scene is due to the contribution of multiple Rayleigh scattering in the simulated spectra, whereas FRESCO+ only includes single Rayleigh scattering.

Next we consider scenes with single-layer and two-layer scattering clouds. Fig. 3 shows the results of the FRESCO and FRESCO+ retrieved cloud heights as a function of solar zenith angle. The FRESCO and FRESCO+ retrieved cloud heights are inside the cloud for a single-layer cloud (Fig. 3a). For a two-layer cloud, FRESCO and FRESCO+ cloud heights are between the two layers (Fig. 3b). The FRESCO and FRESCO+ cloud heights generally increase with increasing SZA, because at large SZA sunlight penetrates less deep into the cloud.

In the single-layer cloud case, the FRESCO cloud heights are almost the same for the fully (c=1) and partly cloudy (c=0.5) scenes. The FRESCO+ cloud height for the partly cloudy scene in Fig. 3a is slightly lower than for the fully cloudy scene. At SZA=45°, the difference between

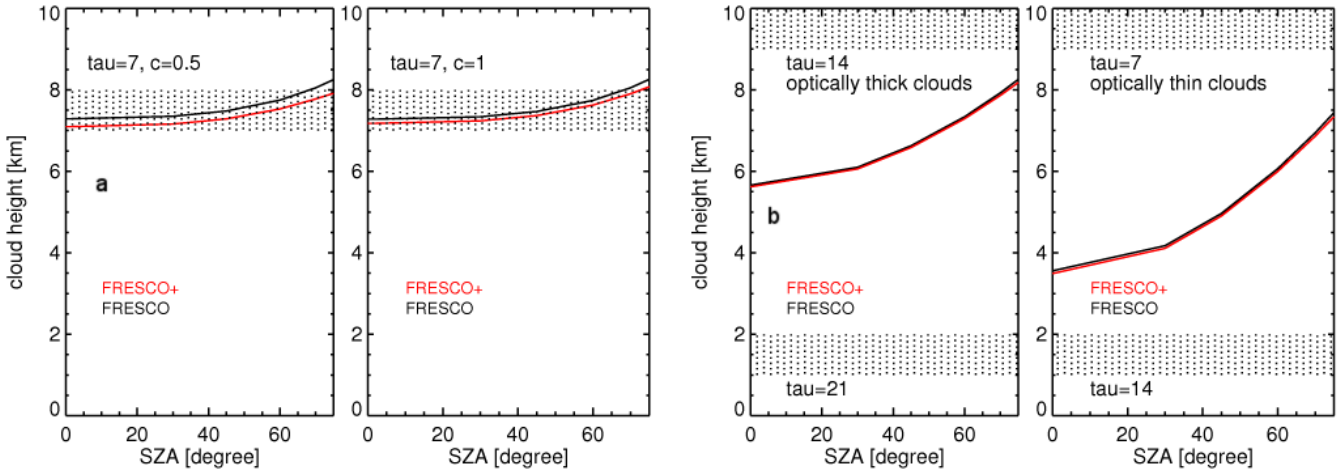

Fig. 3. FRESCO+ and FRESCO retrieved cloud heights using simulated spectra from a line-by-line multiple scattering model. Cases: **(a)** single-layer clouds, optical thickness tau=7, cloud height at 7–8 km, and geometric cloud fraction c=0.5 and 1. **(b)** two-layer clouds, cloud layer 1 at 9–10 km, cloud layer 2 at 1–2 km. Optically thick cloud: tau1=14, tau2=21. Optically thin cloud: tau1=7, tau2=14, geometric cloud fraction c=1.

FRESCO+ and FRESCO cloud heights is –0.1 km for c=1 (c_{eff}=0.4) and –0.2 km for c=0.5 (c_{eff}=0.2) scenes. FRESCO+ cloud heights are lower than FRESCO cloud heights due to inclusion of single Rayleigh scattering, which makes the reflectance of FRESCO+ in the O_2 absorption bands larger than that of FRESCO. To simulate the same reflectance as the scene, FRESCO+ needs more O_2 absorption, therefore the FRESCO+ cloud height is lower than the FRESCO cloud height.

In the two-layer cloud case, the FRESCO and FRESCO+ cloud heights retrieved in the optically thick cloud case is higher than that retrieved in the optically thin cloud case (see Fig. 3b). In the O_2 A-band photons can penetrate to some distance into the clouds. Therefore the retrieved cloud height depends on both the cloud height and the cloud optical thickness. For the two-layer cloud scenes, the FRESCO and FRESCO+ cloud heights are very close because the clouds are optically thicker than that in the single-layer cloud scene, and the effective cloud fractions are between 0.8–1.0. We found that the difference between the FRESCO+ and FRESCO cloud heights decreases with increasing of effective cloud fraction.

3.2 FRESCO+ and FRESCO cloud retrievals from GOME data

The FRESCO+ and FRESCO cloud retrievals have been compared for one month of global GOME data in January 2000. The effective cloud fraction and cloud pressure frequency distributions are shown in Fig. 4. The FRESCO+ and FRESCO effective cloud fraction distributions almost coincide except that FRESCO+ has more clouds at effective cloud fractions 1 and 0. The mean effective cloud fractions differ about 0.01, with FRESCO+ being higher, because the inclusion of single Rayleigh scattering in FRESCO+ leads to a simulated continuum reflectance that is smaller than that simulated by FRESCO. If we would exclude cloud fractions larger than 0.95, where the chi-squares of the O_2 A-band fit are the largest, the effective cloud fraction difference would only be 0.005. In the cloud pressure distributions only pixels with effective cloud fractions larger than 0.1 are selected, and pixels over snow/ice are excluded. The FRESCO+ cloud pressure distribution is shifted to higher pressures as compared to FRESCO (about 50 hPa), but the shapes of the distributions are similar. The distributions of other months show the same behaviour.

To analyze the difference between the FRESCO+ and FRESCO cloud pressures, we show in Fig. 5 these cloud pressures as a function of effective cloud fraction. For effective cloud fractions below 0.05, the cloud pressures retrieved by FRESCO are often 130 hPa – the lower limit of the FRESCO retrieval – which is not a realistic value. Figure 5 shows that the average cloud pressure retrieved by FRESCO in the smallest effective cloud fraction bin [0, 0.02] is about 250 hPa. FRESCO+ retrieves more reasonable cloud pressures than FRESCO, even if the cloud fraction is less than 0.05. On average FRESCO+ cloud pressures are about 50 hPa higher than FRESCO cloud pressures. The difference in cloud pressure between FRESCO and FRESCO+ is larger for the less cloudy pixels than for the fully cloudy pixels, which is due to the larger relative amount of single Rayleigh scattering in the reflectance. The differences found between the FRESCO and FRESCO+ cloud pressures from GOME observations agree with the simulations.

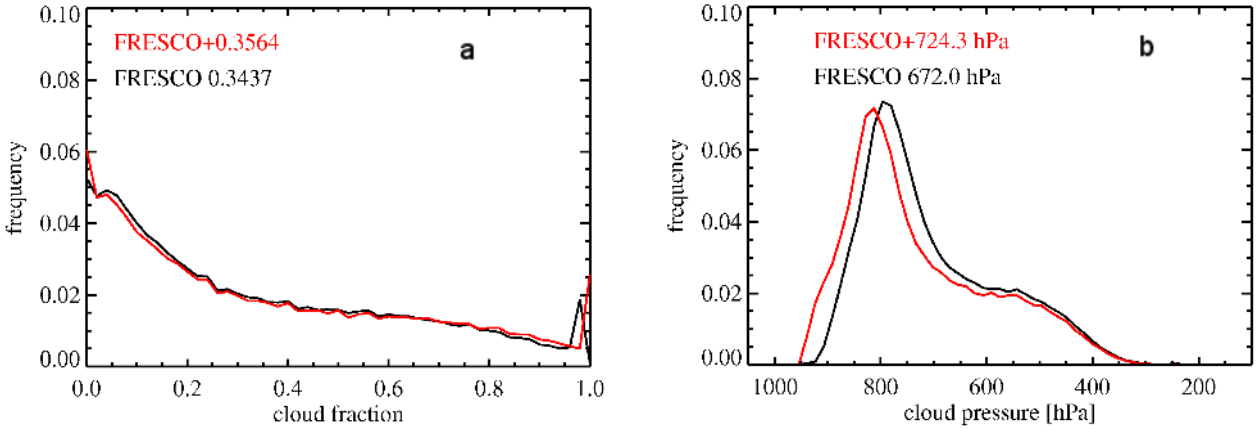

Fig. 4. **(a)** Frequency distributions of FRESCO+ and FRESCO effective cloud fractions for one month of global GOME data in January 2000. **(b)** Same as (a) but for cloud pressures. The distributions are normalized to 1. The average values are given in the legends. The snow/ice pixels are not included in the distributions.

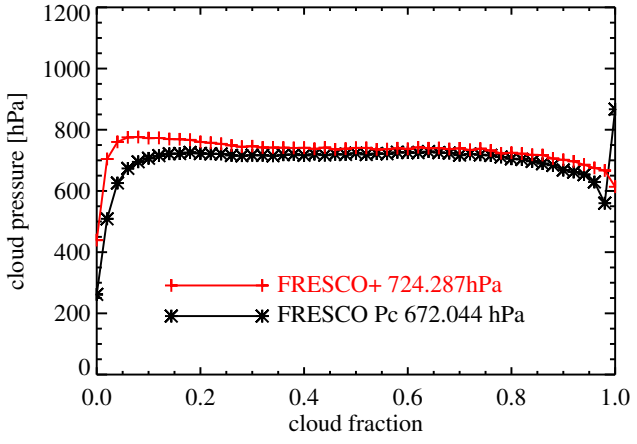

Fig. 5. Cloud pressure from FRESCO+ and FRESCO as a function of effective cloud fraction for the same data as in Fig. 4.

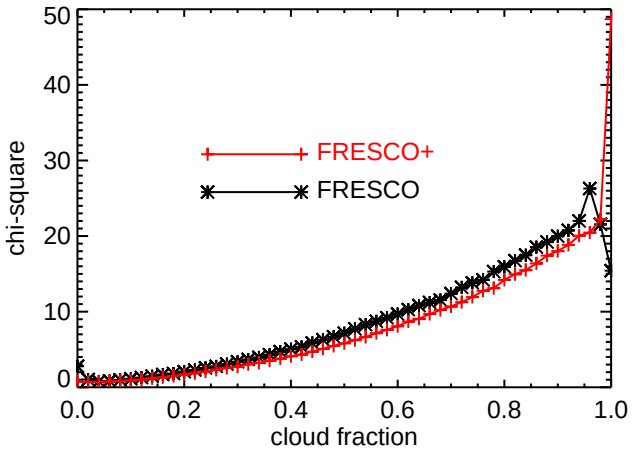

Fig. 6. Chi-square (in arbitrary units) of the O_2 A-band fits from FRESCO+ and FRESCO as a function of effective cloud fraction for the same data as in Fig. 4.

The chi-squares of the FRESCO+ and FRESCO O_2 A-band fits as a function of effective cloud fractions are shown in Fig. 6. The chi-squares of FRESCO+ are smaller than those of FRESCO, which indicates an improvement of the fit in FRESCO+, especially for effective cloud fractions smaller than 0.05. However, when the effective cloud fraction is 1 (i.e. a very bright scene) the chi-squares of FRESCO+ are larger than those of FRESCO. The reason is the following. In both retrieval algorithms the procedure for very bright scenes is: when the measured reflectance at 758 nm is larger than 0.8, the cloud albedo is set to the measured reflectance at 758 nm and the effective cloud fraction is retrieved. If the retrieved effective cloud fraction is larger than 1, it is set to 1 and the chi-square is calculated for c_{eff}=1 but not the retrieved value of c_{eff}>1. In FRESCO+ the simulated transmission in the continuum (T_c in Eq. 1) is smaller than that in FRESCO due to Rayleigh scattering extinction, which is more important at large SZA and for very bright scenes. Therefore, the simulated reflectance by FRESCO+ is smaller than the measured reflectance, which is the reason for the larger chi-squares at c_{eff}=1.

3.3 Validation of FRESCO+ cloud heights with ground-based data

Cloud heights retrieved by FRESCO+ and FRESCO from one year of SCIAMACHY measurements in 2005 have been compared with collocated ARM (Atmospheric Radiation Measurement) active remote sensing cloud boundaries data

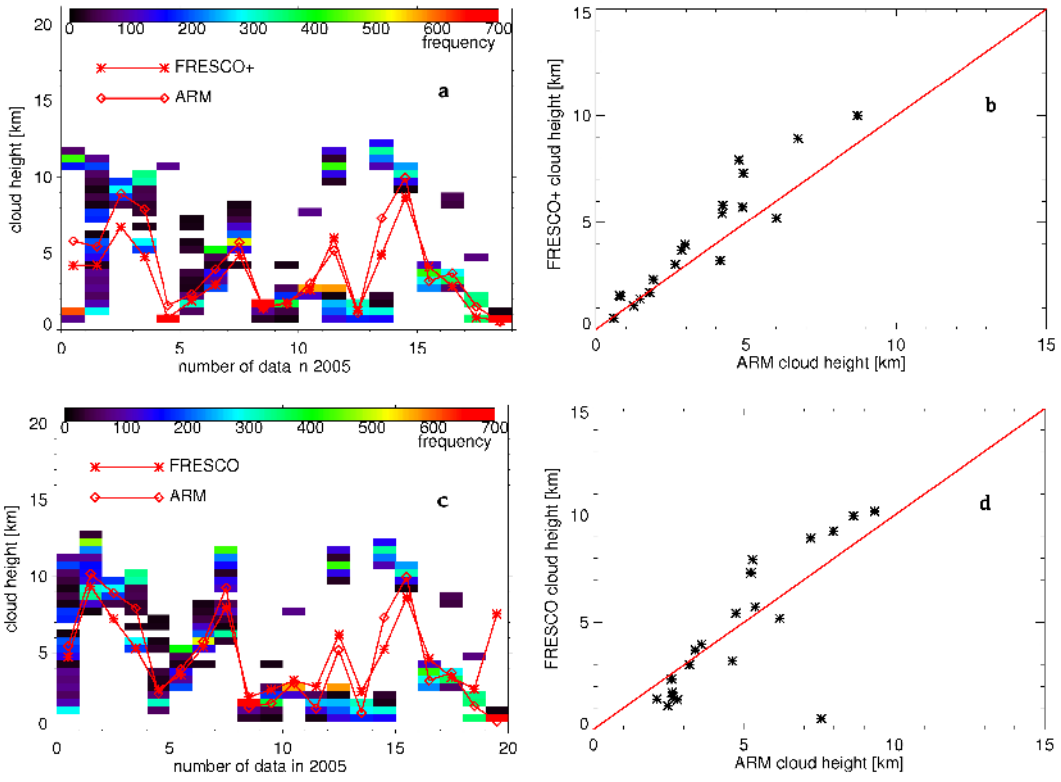

Fig. 7. (a) Comparison between collocated SCIAMACHY FRESCO+ cloud heights and ground-based radar/lidar cloud profiles, for 18 days in 2005 on which SCIAMACHY overpasses of the SGP/ARM site occurred. The color indicates the occurrence of clouds as detected by the radar/lidar. **(b)** Correlation of FRESCO+ cloud height and the average cloud height from the radar/lidar profiles for the same data as in (a), with correlation coefficient of 0.94. **(c)** and **(d)** are similar as (a) and (b) but FRESCO data are used. The correlation coefficient between ARM and FERSCO cloud height is 0.79. Only effective cloud fractions larger than 0.2 are used.

at SGP (Southern Great Plains) in the USA (Clothiaux et al., 2000). The SCIAMACHY pixel size is $30\times60\,\mathrm{km}^2$, which is not easy to compare with ground-based radar/lidar measurements. The criteria we used for spatial and temporal collocation were as follows: (1) the SCIAMACHY data were selected with pixel centers within 60 km of the SGP/ARM site; (2) the SGP/ARM data were selected within one hour of the SCIAMACHY overpass time (10:00 local solar time). The ARM cloud profiles are measured every 10 s with up to 10 cloud layers per measurement. Most measurements have up to 3 cloud layers. The maximum number of collocated cloud data points in one hour is thus 3600. From this data set we calculated the ARM cloud layer height distribution, using the cloud layer heights and their frequency of occurrence.

The ARM cloud layer height distributions and the collocated SCIAMACHY FRESCO+ cloud heights are shown in Fig. 7a. In this plot we have further limited the FRESCO+ effective cloud fractions to values larger than 0.2 and the time periods of ARM cloud cover to periods longer than 30 min, which corresponds to geometric cloud fractions larger than 0.5. As shown in Fig. 7a, the FRESCO+ cloud height is close to the middle of the ARM cloud profiles. This agrees with the results of FRESCO+ for simulated spectra (Sect. 3.1). As shown in Fig. 7b, the FRESCO+ cloud heights have an excellent correlation with the averaged ARM cloud profiles, with a correlation coefficient of 0.94. To demonstrate the improvement in FRESCO+, SCIAMACHY FRESCO and ARM cloud heights are shown in Fig. 7c, d. The criteria used for the selection of SCIAMACHY FRESCO and ARM data are similar as that for FRESCO+ and ARM, except that FRESCO effective cloud fractions are larger than 0.2. The different number of data in FRESCO and FRESCO+ is due to the different FRESCO and FRESCO+ effective cloud fractions. As shown in Fig. 7a, c FRESCO+ retrieves lower cloud height than FRESCO, which agrees with the simulations and the statistic from GOME data. FRESCO+ significantly improves the cloud height retrievals for single-layer low clouds. In this case FRESCO often does not converge and retrieves a cloud height close to the initial value of 5 km. The correlation coefficient of FRESCO and ARM cloud height is 0.79.

4 Impact of FRESCO+ cloud parameters on O_3 and NO_2 retrievals

The FRESCO+ effective cloud fraction and cloud pressure are being used in O_3 and NO_2 total and tropospheric vertical column density (VCD) retrievals performed within the DUE TEMIS project (see http://www.temis.nl). To investigate whether the improvement of the FRESCO+ cloud algorithm also leads to improved trace gas retrievals, we performed the following comparisons: (1) SCIAMACHY total O_3 from the TOSOMI product version 0.4, which uses FRESCO, was compared to version 0.42, which uses FRESCO+; (2) SCIAMACHY total and tropospheric NO_2 column version 1.04, which uses FRESCO, was compared to version 1.1, which uses FRESCO+; (3) a comparison of satellite retrievals using FRESCO+ and FRESCO with ground-based measurements of tropospheric NO_2 was performed.

4.1 Impact of FRESCO+ cloud parameters on total O_3 retrievals

For a partly cloudy pixel the total O_3 vertical column density, N_t, is given by (Van Roozendael et al., 2006):

$$N_t = \frac{N_s + wM_{\text{cloudy}}N_g}{M}, \tag{2}$$

where M is the total air mass factor (AMF) of the partly cloudy pixel, N_s is the measured slant column density, M_{cloudy} is the AMF for a fully cloudy scene, and N_g is the vertical column density below the cloud, which is also called the "ghost column". N_g is computed by integrating the ozone profile from the surface to the cloud pressure level. M is given by the radiance-weighted sum of the AMFs of the clear and cloudy parts of the pixel:

$$M = wM_{\text{cloudy}} + (1-w)M_{\text{clear}}, \tag{3}$$

where w is the weighting factor, and M_{clear} is the AMF for a clear scene. The weighting factor w is the fraction of the photons that originates from the cloudy part of the pixel, and can thus be written as (Martin et al., 2002):

$$w = \frac{cR_{\text{cloudy}}(P_c)}{R}. \tag{4}$$

where c is the (effective) cloud fraction, $R_{\text{cloudy}}(P_c)$ is the average reflectance over the fit window for a scene that is fully covered with a cloud located at pressure P_c, and R is the measured reflectance for the pixel. It is important to mention that in the O_3 and NO_2 retrieval algorithms of TEMIS, clouds are also assumed to be Lambertian reflectors with albedo of 0.8, like in the FRESCO(+) algorithm.

The correlation between the total O_3 vertical column densities retrieved using FRESCO and FRESCO+ cloud products for one day of global SCIAMACHY data is shown in Fig. 8. For this day (10 January 2007) the global averaged

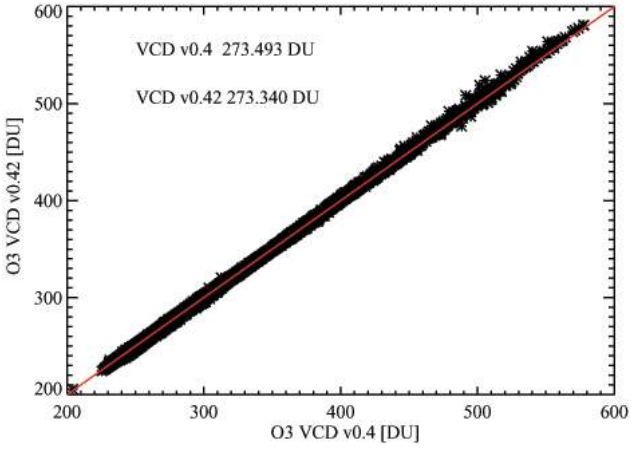

Fig. 8. Correlation of the O_3 vertical column densities for one day of global SCIAMACHY data on 10 January 2007. The O_3 column v0.4 uses FRESCO and the O_3 column v0.42 uses FRESCO+.

difference in O_3 total column is only 0.2 DU. Differences for other days are similar. Apparently, the improvement in the FRESCO+ cloud product has a small effect on total O_3 column retrievals. Since the effective cloud fractions from FRESCO and FRESCO+ are very similar, the difference in the O_3 vertical column is mainly due to the cloud pressure difference. The cloud pressure affects M_{cloudy} and N_g in Eq. 2. The differences between FRESCO+ and FRESCO cloud heights cause only small differences in the total O_3 AMFs and in the ghost columns, because of the relatively low tropospheric O_3 amount. Because O_3 is mainly in stratosphere, the FRESCO+ cloud pressure improvement only weakly affects total O_3 retrieval.

4.2 Impact of FRESCO+ cloud parameters on tropospheric NO_2 retrievals

The cloud correction approaches for the total and tropospheric NO_2 vertical column density retrievals are similar as for the total O_3 retrievals, which are given by Eqs. 2–4. However, the NO_2 air mass factor depends on the NO_2 profile, because a large fraction of NO_2 resides in the troposphere where Rayleigh scattering and scattering by aerosols and clouds are important. Therefore, the tropospheric NO_2 air mass factor M_{tr} is obtained by multiplying the elements of the troposphere-only a-priori NO_2 profile x_a with the elements of the altitude dependent air mass factor m_l as follows (Eskes and Boersma, 2003):

$$M_{tr} = \frac{\sum_l m_l(b) \cdot x_{a,l}}{\sum_l x_{a,l}}, \tag{5}$$

where the elements of the altitude dependent air mass factor depend on the set of model parameters b, including cloud

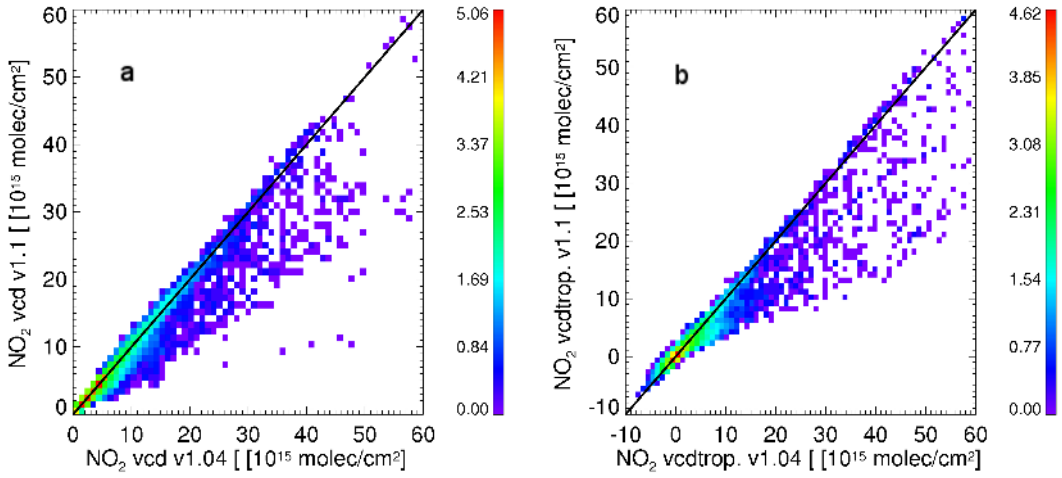

Fig. 9. (a) Correlation of total NO_2 columns using FRESCO+ (v1.1) and using FRESCO (v1.04) for six days of global SCIAMACHY data on 5–10 January 2007. The color scale indicates the density of data points in a logarithm sense. **(b)** Correlation of the tropospheric NO_2 columns for the same SCIAMACHY measurements. The black solid line gives the 1:1 relation between the datasets.

fraction, cloud height and surface albedo. The tropospheric NO_2 VCD is given by:

$$N_{tr} = \frac{N_s - N_{s,st}}{M_{tr}(x_a, b)}. \quad (6)$$

In the TEMIS processing the a-priori NO_2 profile is derived from a chemistry-transport model.

As shown in Fig. 9 both the total NO_2 columns and the tropospheric NO_2 columns retrieved from SCIAMACHY using the FRESCO+ and FRESCO cloud products correlate well. Note that the tropospheric NO_2 VCDs are only reported for pixels with effective cloud fractions less than 0.3. For most of the pixels the NO_2 columns using FRESCO+ and using FRESCO are almost the same, because there is no tropospheric NO_2 or no clouds. Therefore, the globally averaged NO_2 columns are similar. However the largest differences occur for the larger tropospheric NO_2 columns. Similarly Boersma et al. (2007) find that the SCIAMACHY and OMI tropospheric NO_2 columns have large differences at polluted areas. The reason is probably that the OMI cloud heights are lower than FRESCO cloud heights.

The effect of cloud pressure differences on tropospheric NO_2 AMFs and NO_2 ghost columns is shown in Fig. 10. The difference between the ghost columns using FRESCO+ and using FRESCO increases for cloud pressures larger than about 700 hPa; using FRESCO+, the NO_2 ghost columns are clearly smaller than using FRESCO. The difference in tropospheric NO_2 AMFs also increases with cloud pressure; the tropospheric NO_2 AMFs are larger using FRESCO+ than using FRESCO. According to Eq. 2, the increase of AMF and decrease of ghost column both yield a lower tropospheric NO_2 VCD, especially for highly polluted scenes.

We can understand the results of Figs. 9 and 10 as follows. High NO_2 concentrations occur mainly in the boundary layer, roughly below 2 km. For polluted pixels with low clouds even small cloud height differences can cause large differences in NO_2 ghost columns. For polluted pixels with high clouds, when FRESCO and FRESCO+ cloud heights are both above the NO_2 layer, differences in ghost column are small, so differences in NO_2 VCD are also small. The global cloud height frequency distribution from SCIAMACHY shows that the cloud pressure peaks at about 800 hPa. So, globally there are more low clouds than high clouds, and the impact of the FRESCO+ cloud height on tropospheric NO_2 retrievals is significant.

4.3 Comparison with ground-based measurements of tropospheric NO_2

To demonstrate that the FRESCO+ cloud parameters are an improvement for tropospheric NO_2 retrievals from satellite, we compared tropospheric NO_2 columns from SCIAMACHY (v1.1 and v1.04) with ground-based measurements of tropospheric NO_2 columns measured with Multi-AXis DOAS (MAXDOAS) instruments.

The ground-based data include results from the three MAXDOAS instruments (BIRA/IASB, Bremen and Heidelberg) operated during the DANDELIONS (Dutch Aerosol and Nitrogen Dioxide Experiments for vaLIdation of OMI and SCIAMACHY) campaigns held at Cabauw (52° N, 5° E) in May–July 2005 and September 2006. The tropospheric NO_2 VCDs are retrieved using a geometrical approximation valid for boundary-layer NO_2, as described in Brinksma et al. (2008) and subsequently interpolated at the time of the SCIAMACHY overpasses. SCIAMACHY data are selected

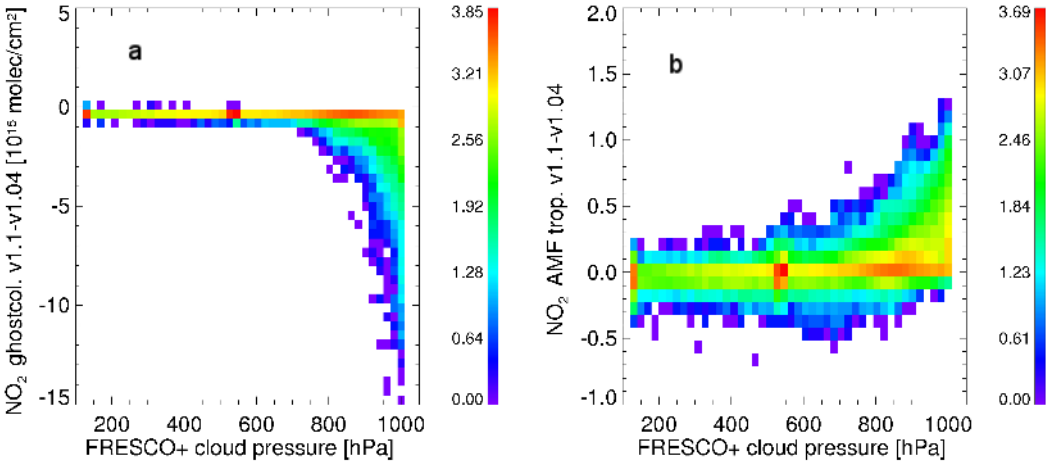

Fig. 10. **(a)** Difference in NO_2 ghost columns between using FRESCO+ clouds (v1.1) and FRESCO clouds (v1.04), as a function of FRESCO+ cloud pressure. **(b)** Similar as (a) but for the difference in tropospheric NO_2 air mass factors. The same SCIAMACHY data as in Fig. 9 were used. The color scale indicates the density of data points in a logarithmic sense.

within a 200 km radius around Cabauw, leading to 72 points of comparison with ground-based measurements. As can be seen in Fig. 11, the distribution of the differences between SCIAMACHY NO_2 VCD retrievals using FRESCO (v1.04) and ground-based measurements is asymmetric, showing more positive deviations. In contrast, the SCIAMACHY NO_2 product using FRESCO+ (v1.1) is closer to the MAXDOAS results, and the differences show a more symmetric distribution. The statistics of the tropospheric NO_2 column differences (SCIAMACHY minus MAXDOAS) are given in Table 1. One can see that the mean and median differences are closer to zero when the FRESCO+ cloud product is used in the SCIAMACHY retrievals. The overall mean difference between the SCIAMACHY NO_2 VCD (v1.1) and ground-based MAXDOAS NO_2 VCD is -2.12×10^{14} molec cm^{-2} with a corresponding standard deviation of 1.02×10^{16} molec cm^{-2}.

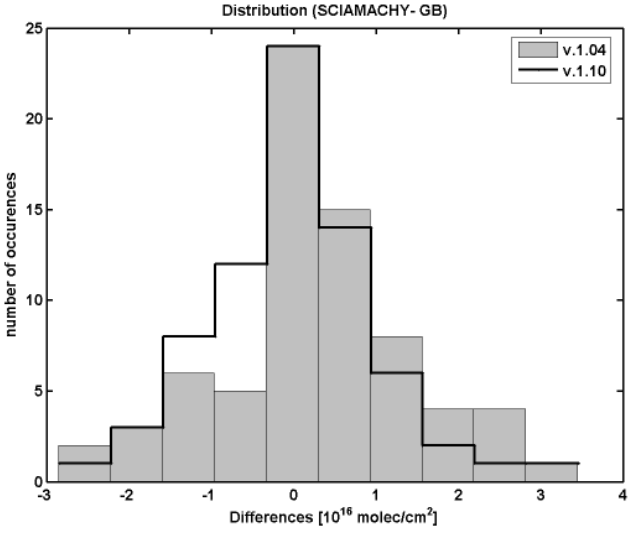

Fig. 11. The distribution of differences between tropospheric NO_2 columns from SCIAMACHY and ground-based MAXDOAS measurements. SCIAMACHY v1.04 uses FRESCO, whereas v1.1 uses FRESCO+.

5 Conclusions

An improved version of the FRESCO cloud algorithm, FRESCO+, has been presented. This version includes Rayleigh scattering which is important for less cloudy scenes. The FRESCO+ algorithm has been applied to simulated O_2 A-band spectra and to GOME and SCIAMACHY satellite measurements of the O_2 A-band spectra. It appears that FRESCO+ yields more accurate cloud heights in less cloudy scenes. The FRESCO+ cloud pressure is about 50 hPa higher in the monthly global average than the FRESCO cloud pressure due to the addition of single Rayleigh scattering. The effective cloud fractions from FRESCO and FRESCO+ differ only by about 0.01 in the monthly global average.

For the first time FRESCO+ cloud height retrievals have been compared to ground-based radar/lidar cloud height measurements and a good correlation was found. From these measurements and simulations we found that the FRESCO+ and FRESCO cloud heights are closer to the middle of the clouds than to the top of the clouds in the scene. This is important to realize when applying FRESCO+ cloud heights in trace gas retrievals and in cloud pressure comparisons.

Table 1. Statistics for tropospheric NO_2 column differences (in units of 1.0×10^{15} molec cm^{-2}) between SCIAMACHY and MAXDOAS measurements, for different effective cloud fraction ranges.

	SCIA FRESCO – MAXDOAS (1.0×10^{15} molec cm^{-2})			SCIA FRESCO+ – MAXDOAS (1.0×10^{15} molec cm^{-2})		
c_{eff} range	Mean	Median	Stddev	Mean	Median	Stddev
≤0.5	2.7	1.9	10.7	−0.91	0.34	8.9
≤1.0	2.8	1.9	11.9	−0.21	0.92	10.2

As a first application we compared the total O_3 columns retrieved from SCIAMACHY using FRESCO+ and FRESCO data in the cloud correction. It appears that the retrieved total O_3 columns are very similar using FRESCO+ or FRESCO cloud products (0.2 DU difference), because the cloud height improvement of FRESCO+ weakly affects stratospheric trace gas retrievals. As a second application, we applied FRESCO+ to NO_2 retrievals from SCIAMACHY. Here we found a large impact of the FRESCO+ on tropospheric NO_2 retrievals. The cloud height improvement influences the ghost column of tropospheric NO_2 directly, especially for highly polluted cases. The cloud height improvement also affects the tropospheric NO_2 air mass factors, because they depend on the NO_2 profile and the profile of the scatterers.

Finally, we compared SCIAMACHY tropospheric NO_2 column retrievals using FRESCO+ and FRESCO to ground-based MAXDOAS measurements performed during the DANDELIONS campaign in Cabauw. We found that the SCIAMACHY tropospheric NO_2 columns using the FRESCO+ cloud product in the cloud correction, agree better with the ground-based data than using the FRESCO cloud product. We conclude that FRESCO+ is an improvement of FRESCO algorithm, not only in the physics of the retrieval algorithm, but also in the application of the cloud product for tropospheric trace gas retrievals.

Appendix A

In this appendix, the formulae for the FRESCO+ simulations of the O_2 A-band reflectance are given, which is an update of the FRESCO formulae given by Koelemeijer et al. (2001).

A1 Rayleigh scattering cross section and phase function

The Rayleigh scattering cross section, σ_R, is calculated with the formula (Bates, 1984):

$$\sigma_R = (32\pi^3/3N^2\lambda^4)(n_{\text{air}}-1)^2 F'_k(\text{air}), \tag{A1}$$

where $(n_{\text{air}}-1)$ is the refractive index, and $F'_k(\text{air})$ is the effective King correction factor. The effective King correction factors and refractive index for air are chosen at 750 and 800 nm from Table 1 in Bates (1984), and are linearly interpolated between 750 and 800 nm.

The Rayleigh scattering phase function (without polarization) is given by

$$F_R(\Theta) = \frac{3(1-\rho_n)}{4(1+\rho_n/2)}(\cos^2\Theta + \frac{1+\rho_n}{1-\rho_n}), \tag{A2}$$

with

$$\cos\Theta = -\cos\theta\cos\theta_0 + \sin\theta\sin\theta_0\cos(\varphi-\varphi_0), \tag{A3}$$

where Θ is the scattering angle, θ is the viewing zenith angle, θ_0 is the solar zenith angle, φ is the viewing azimuth angle, and φ_0 is the solar azimuth angle. ρ_n is the depolarization factor; at 750 nm ρ_n=0.02786.

A2 Atmospheric optical thickness and transmission

The atmospheric optical thickness and transmission is determined by oxygen absorption and Rayleigh scattering. The absorption is calculated from the number density of O_2 molecules (n_{O_2}) and the O_2 absorption cross section, $\sigma_{O_2}(\lambda)$, along the light path. $\sigma_{O_2}(\lambda)$ depends on the atmospheric temperature and pressure but this is omitted from the notation. The absorption coefficient (in 1/m) is given by:

$$k_{\text{abs}}(\lambda, z) = n_{O_2}(z)\sigma_{O_2}(\lambda, z). \tag{A4}$$

The Rayleigh scattering coefficient is calculated from the air density (n_{air}) and the Rayleigh scattering cross section ($\sigma_R(\lambda, z)$),

$$k_{\text{sca}}(\lambda, z) = n_{\text{air}}(z)\sigma_R(\lambda, z). \tag{A5}$$

The total atmospheric optical thickness, τ, is the sum of the absorption and scattering contributions:

$$\tau(\lambda, z_r, \theta, \theta_0) = \int_{z_r}^{\infty}(k_{\text{abs}}(\lambda, z+k_{\text{sca}}(\lambda, z))(S_{\text{sp}}(\theta_0, z-z_r)+S_{\text{sp}}(\theta, z-z_r))dz. \tag{A6}$$

Here $S_{\text{sp}}(\theta_0, z-z_r)$ and $S_{\text{sp}}(\theta, z-z_r)$ are the spherical light path factors from the sun to the reflector and from the reflector to the satellite (Koelemeijer et al., 2001). z is height in the atmosphere, z_r is the altitude of the reflector (surface

or clouds). θ_0, θ are the solar zenith angle and viewing zenith angle at surface height.

The transmittance from TOA to z_r, assuming a reflector at altitude z_r, and back from z_r to TOA is now given by:

$$T(\lambda, z_r, \theta, \theta_0) = e^{-\tau(\lambda, z_r, \theta, \theta_0)}. \quad \text{(A7)}$$

The transmittances T are stored in a look-up-table (LUT).

A3 Single Rayleigh scattering reflectance

The single Rayleigh scattering reflectance, R_R, is calculated with the formula (see Fig. 2) (Hovenier et al., 2005),

$$R_R(\lambda, z_r, \mu, \mu_0, \varphi - \varphi_0) = \frac{F_R(\mu, \mu_0, \varphi - \varphi_0)}{4\mu_0\mu} \int_{z_r}^{\infty} k_{\text{sca}}(\lambda, z) T(\lambda, z, \mu, \mu_0) dz, \quad \text{(A8)}$$

where $T(\lambda, z, \mu, \mu_0)$ is the transmittance, $\mu_0 = \cos\theta_0$, $\mu = \cos\theta$. We have to modify Eq. A8 for the spherical light path:

$$R_R(\lambda, z_r, \theta, \theta_0, \varphi - \varphi_0) = \frac{F_R(\theta, \theta_0, \varphi - \varphi_0)}{4\cos\theta_0} \int_{z_r}^{\infty} k_{\text{sca}}(\lambda, z) T(\lambda, z, \theta, \theta_0) S_{\text{sp}}(\theta, z) dz. \quad \text{(A9)}$$

Since we can neglect the wavelength dependence of the Rayleigh scattering phase function F_R in the O_2 A-band, we can multiply by the phase function in Eq. A9 after the convolution with the slit function. Therefore, the reflectances are stored in a look-up-table (LUT) as:

$$R_1(\lambda, z_r, \theta, \theta_0) = \int_{z_r}^{\infty} k_{\text{sca}}(\lambda, z) T(\lambda, z, \theta, \theta_0) S_{\text{sp}}(\theta, z) dz. \quad \text{(A10)}$$

Another advantage of using Eq. A10 is that the azimuth is not needed in the reflectance LUT, which now has the same parameters as the FRESCO+ transmittance LUT. The factor $F_R(\theta, \theta_0, \varphi - \varphi_0)/(4\cos\theta_0)$ is calculated in the FRESCO+ retrieval program according to the measurement geometry. In the main text, R_s and R_c are R_R for clear sky and cloudy cases, respectively. $R_c = R_R(\lambda, z_c, \theta, \theta_0, \varphi - \varphi_0)$, $R_s = R_R(\lambda, z_s, \theta, \theta_0, \varphi - \varphi_0)$, where z_c is the cloud height, and z_s is the surface height.

Acknowledgements. Funding was provided by the Netherlands Institute for Space Research (SRON) through the FRESCO+ project (EO-067). SCIAMACHY validation activities at BIRA-IASB are funded by the PRODEX CINAMON project. The MAXDOAS measurements during the DANDELIONS campaign were supported by the EU FP6, through the ACCENT NoE. ARM data is made available through the US Department of Energy as part of the Atmospheric Radiation Measurement Program.

Edited by: J. Quaas

References

Bates, D. R.: Rayleigh scattering by air, Planet. Space Sci., 32(6), 785–790, 1984.

Brinksma, E. J., Pinardi, G., Braak, R. et al.: The 2005 and 2006 DANDELIONS NO_2 and aerosol intercomparison campaigns, J. Geophys. Res., 113, D16S46, doi:10.1029/2007JD008808, 2008.

Boersma, K. F., Eskes, H. J., Veefkind, J. P., Brinksma, E. J., van der A, R. J., Sneep, M., van den Oord, G. H. J., Levelt, P. F., Stammes, P., Gleason, J. F., and Bucsela, E. J.: Near-real time retrieval of tropospheric NO_2 from OMI, Atmos. Chem. Phys., 7, 2103–2118, 2007, http://www.atmos-chem-phys.net/7/2103/2007/.

Clothiaux, E. E., Ackerman, T. P., Mace, G. G., Moran, K. P., Marchand, R. T., Miller, M. A. and Martner, B. E.: Objective determination of cloud heights and radar reflectivities using a combination of active remote sensors at the ARM CART sites, J. Appl. Meteorol., 39, 645–665, 2000.

van Diedenhoven, B., Hasekamp, O. P., and Landgraf, J.: Retrieval of cloud parameters from satellite-based reflectance measurements in the ultraviolet and the oxygen A-band, J. Geophys. Res., 112, D15208, doi:10.1029/2006JD008155, 2007.

Eskes, H. J. and Boersma, H. F.: Averaging kernels for DOAS total-column satellite retrievals Atmos. Chem. Phys. 3, 1285–1291, 2003.

Fournier, N., Stammes, P., de Graaf, M., van der A, R., Piters, A., Grzegorski, M., and Kokhanovsky, A.: Improving cloud information over deserts from SCIAMACHY Oxygen A-band measurements, Atmos. Chem. Phys., 6, 163–172, 2006, http://www.atmos-chem-phys.net/6/163/2006/.

Grzegorski, M., Wenig, M., Platt, U., Stammes, P., Fournier, N., and Wagner, T.: The Heidelberg iterative cloud retrieval utilities (HICRU) and its application to GOME data, Atmos. Chem. Phys., 6, 4461–4476, 2006, http://www.atmos-chem-phys.net/6/4461/2006/.

de Haan, J. F., Bosma, P. B., and Hovenier, J. W.: The adding method for multiple scattering calculations of polarized light, Astron. Astrophys., 183, 371–391,1987.

Hovenier, J. W., Domke, H., and van der Mee, C.: Transfer of Polarized Light in Planetary Atmospheres: Basic Concepts and Practical Methods, Kluwer academic publishers, Dordrecht/Boston/London, 2005.

Koelemeijer, R. B. A. and Stammes, P.: Effects of clouds on the ozone column retrieval from GOME UV measurements, J. Geophys. Res., D104, 8281–8294, 1999.

Koelemeijer, R. B. A., Stammes, P., Hovenier, J. W., and de Haan, J. F.: A fast method for retrieval of cloud parameters using oxygen A-band measurements from the Global Ozone Monitoring Experiment, J. Geophys. Res., 106, 3475–3490, 2001.

Koelemeijer, R. B. A., de Haan, J. F., and Stammes, P.: A database of spectral surface reflectivity in the range 335–772 nm derived from 5.5 years of GOME observations, J. Geophys. Res., 108(D2), D24070, doi:10.1029/2002JD002429, 2003.

Kokhanovsky, A. A., Rozanov, V. V., Nauss, T., Reudenbach, C., Daniel, J. S., Miller, H. L., and Burrows, J. P.: The semianalytical cloud retrieval algorithm for SCIAMACHY I. The validation, Atmos. Chem. Phys., 6, 1905–1911, 2006, http://www.atmos-chem-phys.net/6/1905/2006/.

Krijger, J. M., van Weele, M., Aben, I., and Frey, R.: Technical

Note: The effect of sensor resolution on the number of cloud-free observations from space, Atmos. Chem. Phys., 7, 2881–2891, 2007,
http://www.atmos-chem-phys.net/7/2881/2007/.

Loyola, D.: Automatic cloud analysis from polar-orbiting satellites using neural network and data fusion techniques, in: proceedings of the IEEE international geoscience and remote sensing symposium, IGARSS'2004, Anchorage, 4, 2530–2534, 2004.

Martin, R. V., Chance, K., Jacob, D. J., et al.: An improved retrieval of tropospheric Nitrogen Dioxide from GOME, J. Geophys. Res., 107(D20), 4437, doi:10.1029/2001JD001027, 2002.

Munro, R. and Eisinger, M.: The Second Global Ozone Monitoring Experiment (GOME-2) An Overview, programme development department technical memorandum No. 11, Eumetsat, Darmstadt, October 2004.

Rothman, L. S., Jacquemart, D., Barbe, A., et al.: The HITRAN 2004 molecular spectroscopic database, Journal of Quantitative Spectroscopy and Radiative Transfer 96, 139–204, 2005.

Stammes, P., de Haan, J., and Hovenier, J.: The polarized internal radiation field of a planetary atmosphere, Astron. Astrophys., 225, 239–259, 1989.

Stammes, P.: Spectral radiance modeling in the UV-visible range, in: IRS 2000: Current Problems in Atmospheric Radiation, edited by: Smith, W. and Timofeyev, Y., 385–388, A. Deepak, Hampton, Va., 2001.

Stammes, P., Sneep M., de Haan, J. F., Veefkind, J. P., Wang, P., and Levelt, P. F.: Effective cloud fractions from OMI: theoretical framework and validation, J. Geophys. Res., 113, D16S38, doi:10.1029/2007JD008820, 2008.

Tuinder, O. N. E., de Winter-Sorkina, R., and Builtjes, P. J. H.: Retrieval methods of effective cloud cover from the GOME instrument: an intercomparison, Atmos. Chem. Phys., 4, 255–273, 2004,
http://www.atmos-chem-phys.net/4/255/2004/.

Van Roozendael, M., Loyola, D., Spurr, R., Balis, D., Lambert, J.-C., Livschitz, Y., Valks, P., Ruppert, T., Kenter, P., Fayt, C., and Zehner, C.: Ten years of GOME/ERS-2 total ozone data-The new GOME data processor (GDP) version 4: 1. Algorithm description, J. Geophys. Res., 111, D14311, doi:10.1029/2005JD006375, 2006.

Wang, P., Stammes, P., and Boersma, K. F.: Impact of the effective cloud fraction assumption on tropospheric NO_2 retrievals, in Proceedings of the First Conference on Atmospheric Science, Eur. Space Agency Spec. Publ., ESA SP-628, 4–38, 2006.

Wang, P. and Stammes, P.: FRESCO-GOME2 project, EUM/CO/06/1536/FM, final report, Eumetsat, Darmstadt, 14 September, 2007.